Correspondence

Acoustic Scattering of an Incident Cylindrical Wave by an Infinite Circular Cylinder

T. J. CAVICCHI AND W. D. O'BRIEN, JR.

Abstract—**Exact scattered acoustic fields generated by an infinite circular cylinder in the presence of an incident cylindrical wave are derived for fluid media. Equations are given for the scattered field outside the cylinder and for the total field within.**

This note contains a derivation of the exact fields in fluid media associated with an infinite cylinder of circular cross section in the presence of an incident cylindrical wave. Exact expressions for the scattered field from a cylinder exposed to a plane wave are well known [3], [4]. The problem was solved for a rigid cylinder exposed to a cylindrical wave in 1962 [5]. For the electromagnetic case of a conducting cylinder, scattered fields only outside the cylinder were derived [6], and can be shown to be mathematically equivalent to the corresponding expression given here. Expressions for the case of acoustic scattering in elastic solid cylindrical media appear in [2]. A result for the acoustic case (again, only for the exterior region) for fluid media appears in [1], but it has an erroneous factor of i^m in the series expansion in [1, Eq. (2.24)]. (This is borne out analytically in the present derivation. Numerically, it was also verified, in that the scattered field expressions given in this paper computationally satisfy the condition of continuous pressure across the cylinder boundary. However, use of their [1, Eq. (2.25)], which is essentially correct, in [1, Eq. (2.24)] with the analogously derived expression for the internal field including the i^m factor do not. Further numerical verification of the validity of the formulas presented here can be found in [2], where use of these formulas led to successful tomographic reconstructions of cylinders.) For computer tomography simulations [2], it is useful to have available the scattered field at selected points outside the cylinder. Also, testing of reconstruction algorithms can make use of exact field distributions within the object region, and consequently inside the cylinder. Therefore, it is helpful to have available the total field at any desired point in space. Such expressions are derived here.

Because the circular cylinder is symmetric, clearly all that needs to be specified geometrically is the angle ϕ between transmitter and detector and the radii of the detector and transmitter measured from the cylinder center; the coordinate system can be aligned with the transmitter-cylinder center line (see Fig. 1)). The wave equation in polar coordinates is

$$\partial^2 f/\partial t^2 = c^2\nabla^2 f = c^2/r[\partial/\partial r(r\partial f/\partial r) + (1/r)\,\partial^2 f/\partial\phi^2]. \quad (1)$$

Assuming time dependence $e^{i\omega t}$ the general solution to (1) is

$$f(r, \phi, t) = \sum_{m=0}^{\infty} \{A_m J_m(kr) + B_m Y_m(kr)\} \cos(m\phi)\, e^{i\omega t}, \quad (2)$$

Manuscript received September 4, 1986; accepted December 15, 1986. This work supported in part by the NIH Oncology Training Fellowship CA 09067, and in part by NIH CA 36029.

The authors are with the Bioacoustics Research Laboratory, Department of Electrical and Computer Engineering, University of Illinois, 1406 Green St., Urbana, IL 61801.

IEEE Log Number 8717134.

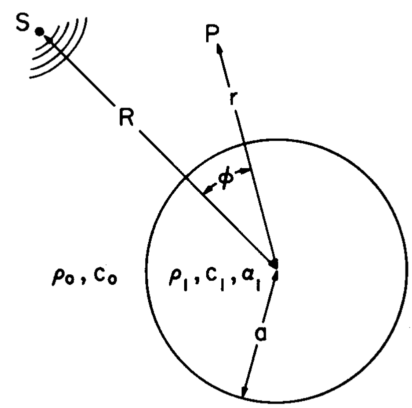

Fig. 1. Geometry for scattering of a cylindrical wave by an infinite circular cylinder of radius a, density ρ_1, speed of sound c_1, and absorption coefficient α_1 in lossless, homogeneous space of density ρ_0 and speed of sound c_0. Radii from the cylinder enter to the source S and observation point P are of lengths R and r, respectively, and diverge by angle ϕ.

where:

A_m and B_m	are complex weighting coefficients;
$J_m(kr)$ and $Y_m(kr)$	are Bessel functions of the first and second kinds, respectively;
$\cos(m\phi)$	is the angular function. Cos $(m\phi)$ can be used instead of $e^{im\phi}$ because the problem is symmetric with respect to the $\phi = 0$ line.

Let ρ_1 and ρ_0, c_1 and c_0, and k_1 and k_0 be, respectively, the densities, sound velocities, and wavenumbers inside and outside the cylinder. Equation (1) must be solved separately inside the cylinder ($f = f^w$) and outside ($f = f^{sc} + f^{inc}$). In order to match boundary conditions, the representation of the incident cylindrical wave (centered on the source) must be changed from one with the source point as the origin (in which case we have the representation $f^{inc} = H_0^{(2)}(k_0 r_s)$ to one with the center of the cylinder as the origin. Here r_s is the distance between the desired point of evaluation and the line (cylindrical point) source and in general, $H_m^{(2)}(x) = J_m(x) - iY_m(x)$ is the mth order Hankel function of the second kind. If ϕ designates the angle between the source-cylinder center line and the source-observation point line, and R the distance from the source to origin (=cylinder center), the addition theorem for Bessel functions states that for any Bessel function $Z(kr)$,

$$e^{in\phi} Z_n(kr) = \sum_{m=-\infty}^{\infty} J_m(kr)\, Z_{m+n}(kR)\, e^{im\phi}, \quad (3)$$

where on the right hand side r is measured in the new coordinate system. In our case, $n = 0$ and Z is $H^{(2)}$ ($H_0^{(2)}$ is what we want to expand). Therefore our specialization of (3) is

$$Z_0(kr) = \sum_{m=-\infty}^{\infty} J_m(kr)\, Z_m(kR)\, e^{im\phi}. \quad (4)$$

Assuming a unity amplitude source and dropping the $e^{i\omega t}$ factor, and again noting symmetry about the line $\phi = 0$, the incident field can be written as

$$f^{inc}(r, \phi) = \sum_{m=-\infty}^{\infty} J_m(k_0 r)\, H_m^{(2)}(k_0 R) \cos(m\phi). \tag{5}$$

For computation, it will be convenient to express (5) as a sum from $m = 0$ to ∞, rather than $-\infty$ to $+\infty$. Using the identity

$$Z_{-n}(x) = (-1)^n Z_n(x), \tag{6}$$

which is true for n an integer, (5) can be rewritten as

$$f^{inc}(r, \phi) = J_0(k_0 r)\, H_0^{(2)}(k_0 R) + \sum_{m=1}^{\infty} J_m(k_0 r)\, H_m^{(2)}(k_0 R) \cdot \left(1 + (-1)^{2m}\right) \cos(m\phi), \tag{7a}$$

or

$$f^{inc}(r, \phi) = J_0(k_0 r)\, H_0^{(2)}(k_0 R) + 2 \sum_{m=1}^{\infty} J_m(k_0 r)\, H_m^{(2)}(k_0 R) \cos(m\phi). \tag{7b}$$

Similarly, the scattered field can be written as

$$f^{sc}(r, \phi) = \sum_{m=0}^{\infty} S_m H_m^{(2)}(k_0 r) \cos(m\phi) \qquad (r \geq a), \tag{8}$$

and the field within the cylinder as

$$f^{w}(r, \phi) = \sum_{m=0}^{\infty} W_m J_m(k_1 r) \cos(m\phi) \qquad (0 \leq r \leq a). \tag{9}$$

Now terms can be equated when the boundary conditions are enforced because all of the above expressions have the same form.

In the previous equations the f's denote pressure fields. Keeping this in mind in the following discussion of boundary conditions, the acoustic linear equation of motion can be written

$$\rho \partial \vec{u} / \partial t = -\nabla f \tag{10}$$

where $\vec{u}$ is the particle velocity and ρ is the density. For the two-dimensional case in cylindrical coordinates, (10) becomes

$$\rho \partial \vec{u} / \partial t = -\left(\hat{r} \partial f / \partial r + \hat{\phi}(1/r)\, \partial f / \partial \phi\right), \tag{11}$$

where $\vec{u} = \hat{r} u_r + \hat{\phi} u_\phi$.

The boundary condition involving velocity is the continuity of u_r—thus only u_r needs to be calculated and not u_ϕ. The equation for u_r is, from (11) and the $e^{i\omega t}$ time dependence,

$$i\omega\rho u_r = -\partial f / \partial r \quad \text{or} \quad u_r = (i/\omega\rho)\, \partial f / \partial r \tag{12}$$

Now the incident field radial velocity u_r^{inc} is calculated

$$u_r^{inc}(r, \phi) = (i/\omega\rho_0) \left(H_0^{(2)}(k_0 R)\, \partial/\partial r(J_0(k_0 r)) + 2 \sum_{m=1}^{\infty} \left\{ H_m^{(2)}(k_0 R)\, \partial/\partial r(J_m(k_0 r)) \cos(m\phi) \right\} \right). \tag{13}$$

Using the identity

$$d/dx(Z_m(x)) = 1/2(Z_{m-1}(x) - Z_{m+1}(x)), \tag{14}$$

and (6),

$$\partial/\partial r(Z_0(k_0 r)) = (k_0/2)[Z_{-1}(k_0 r) - Z_1(k_0 r)] = -k_0 Z_1(k_0 r) \tag{15a}$$

$$\partial/\partial r(Z_m(k_0 r)) = (k_0/2)[Z_{m-1}(k_0 r) - Z_{m+1}(k_0 r)], \tag{15b}$$

so (13) becomes, for the incident field radial velocity,

$$u_r^{inc}(r, \phi) = -i/Z_0 \left(H_0^{(2)}(k_0 R)\, J_1(k_0 r) + \sum_{m=1}^{\infty} \left\{ H_m^{(2)}(k_0 R)[J_{m+1}(k_0 r) - J_{m-1}(k_0 r)] \cos(m\phi) \right\} \right) \tag{16}$$

where $k_0 = \omega / c_0$ and henceforth Z refers to acoustic impedance so $Z_0 = \rho_0 c_0$. Use of (14) is made for concreteness, in that the results contain only easily obtainable functions in a computational setting.

Similarly, for the scattered field radial velocity,

$$u_r^{sc}(r, \phi) = (i/\omega\rho_0) \left(S_0 \partial/\partial r(H_0^{(2)}(k_0 r)) + \sum_{m=1}^{\infty} \left\{ S_m \partial/\partial r(H_m^{(2)}(k_0 r)) \cos(m\phi) \right\} \right) \tag{17a}$$

$$u_r^{sc}(r, \phi) = -(i/Z_0) \left(S_0 H_1^{(2)}(k_0 r) + \sum_{m=1}^{\infty} \left\{ (S_m/2)[H_{m+1}^{(2)}(k_0 r) - H_{m-1}^{(2)}(k_0 r)] \cos(m\phi) \right\} \right) \tag{17b}$$

Now the internal field radial velocity can immediately be written

$$u_r^{w}(r, \phi) = -(i/Z_1) \cdot \left(W_0 J_1(k_1 r) + \sum_{m=1}^{\infty} \left\{ (W_m/2)[J_{m+1}(k_1 r) - J_{m-1}(k_1 r)] \cos(m\phi) \right\} \right) \tag{18}$$

where $Z_1 = \rho_1 c_1$ for lossless cylinders and $Z_1 = \rho_1 c_1 / [1 - i(\alpha_1 c_1 / \omega)]$ for lossy cylinders, where α_1 is the pressure absorption coefficient within the cylinder.

Now the two boundary conditions may be applied:

1) continuous pressure across the cylinder boundary $r = a$, where a is the cylinder radius,

$$f^{w}(r = a, \phi) = f^{sc}(r = a, \phi) + f^{inc}(r = a, \phi); \tag{19}$$

2) continuous radial velocity across the cylinder boundary

$$u_r^{w}(r = a, \phi) = u_r^{sc}(r = a, \phi) + u_r^{inc}(r = a, \phi). \tag{20}$$

First consider the case $m = 0$.

Boundary condition (1) reads

$$W_0 J_0(k_1 a) = S_0 H_0^{(2)}(k_0 a) + J_0(k_0 a)\, H_0^{(2)}(k_0 R) \tag{21}$$

and boundary condition 2) reads (with division by $-i$)

$$(1/Z_1)\, W_0 J_1(k_1 a) = (1/Z_0)[S_0 H_1^{(2)}(k_0 a) + H_0^{(2)}(k_0 R)\, J_1(k_0 a)] \tag{22}$$

The solution for S_0 is

$$S_0 = (-1/\Delta_0)[J_1(k_0 a)\, J_0(k_1 a) - J_0(k_0 a)\, J_1(k_1 a)\, Z_r]\, H_0^{(2)}(k_0 R) \tag{23}$$

and the solution for W_0 is

$$W_0 = (1/\Delta_0)[H_1^{(2)}(k_0 a)\, J_0(k_0 a) - H_0^{(2)}(k_0 a)\, J_1(k_0 a)]\, H_0^{(2)}(k_0 R) \tag{24}$$

where

$$\Delta_0 = H_1^{(2)}(k_0 a)\, J_0(k_1 a) - H_0^{(2)}(k_0 a)\, J_1(k_1 a)\, Z_r \tag{25}$$

where $Z_r = Z_0 / Z_1$.

Note: the above formulas are identical to those for the W_0 and S_0($m = 0$ weights) for an incident plane wave (remember, our incident wave is cylindrical) except for the factor $H_0^{(2)}(k_0 R)$. This is obvious because in the incident field expansion, the two zero-order terms also differ by only the same factor.

Now consider $m > 0$. The only difference between the boundary conditions for this case and the case $m = 0$ is that all zero orders are replaced by m orders and the terms from the incident field for the $m > 0$ case are twice those of the $m = 0$ case.

The solution for S_m is

$$S_m = (-2/\Delta_m)\, H_m^{(2)}(k_0 R) \left\{ J_m(k_1 a)[J_{m+1}(k_0 a) - J_{m-1}(k_0 a)] - J_m(k_0 a)[J_{m+1}(k_1 a) - J_{m-1}(k_1 a)]\, Z_r \right\} \tag{26}$$

where

$$\Delta_m = J_m(k_1a)\left[H_{m+1}^{(2)}(k_0a) - H_{m-1}^{(2)}(k_0a)\right] - H_m^{(2)}(k_0a)\left[J_{m+1}(k_1a) - J_{m-1}(k_1a)\right] Z_r. \quad (27)$$

Finally, the solution for W_m is

$$W_m = (2/\Delta_m)\, H_m^{(2)}(k_0R)\left\{J_m(k_0a)\left[H_{m+1}^{(2)}(k_0a) - H_{m-1}^{(2)}(k_0a)\right] - H_m^{(2)}(k_0a)\left[J_{m+1}(k_0a) - J_{m-1}(k_0a)\right]\right\}. \quad (28)$$

Again, the weighting coefficients differ from those for an incident plane wave by only a factor of $(i^{-m}) \cdot H_m^{(2)}(k_0R)$.

References

[1] M. Azimi, A. C. Kak, "Multiple scattering and attenuation phenomena in diffraction tomography," Purdue Univ. Tech. Report TR-EE 85-4, p. 16, 1985.

[2] T. J. Cavicchi, S. A. Johnson, and W. D. O'Brien, Jr., "Application of the sinc basis moment method to the reconstruction of infinite circular cylinders," *IEEE Trans. Ultrason. Ferroelect. Freq. Contr.*, this issue, pp. 22-33.

[2] A. L. Fang, "Scattering of a cylindrical wave of sound by an elastic cylinder," *Acustica*, vol. 13, no. 6, pp. 397-402, 1963.

[3] L. A. Longley, W. D. O'Brien, Jr., "Ultrasonic heating distributions in lossy cylinders and spheres," *IEEE Trans. Sonics Ultrason.*, vol. SU-29, no. 2, pp. 69-78, Mar. 1982.

[4] P. M. Morse, K. U. Ingard, *Theoretical Acoustics*. New York: McGraw-Hill, 1968, ch. 8.

[5] E. L. Shenderov, "Diffraction of a cylindrical wave by a cylinder," *Soviet Physics-Acoustics*, vol. 7, no. 3, pp. 293-296, Jan.-Mar. 1962.

[6] J. R. Wait, "The cylindrical ore body in the presence of a cable carrying an oscillating current," *Geophysics*, vol. 17, no. 2, pp. 378-386, 1952.

Thin-Film Ferroelectrics of PZT by Sol–Gel Processing

S. K. DEY, K. D. BUDD, AND D. A. PAYNE

Abstract—**The ferroelectric effect has been demonstrated for sol-gel derived PZT (53/47) thin films. The respective values of coercive field and remanent polarization were 4.10^6 V/m and 0.36 C/m^2. The thin film fabrication process is simple and compatible with Si planar technology, and offers a wide variety of potential uses for counting, memory and, integrated optical circuit applications.**

Introduction

Recently, there has been considerable interest in the processing of ferroelectrics in thin-film form due to the growing demand for compatibility with integrated circuit (IC) planar technology. Thin-film ferroelectrics would have lower operating voltages, reduced sizes; and sol-gel processing is a relatively inexpensive method that is compatible with a variety of substrate materials.

Crystalline solutions in the lead zirconate ($PbZrO_3$)-lead titanate ($PbTiO_3$) system (i.e., PZT), in bulk form, have high permittivites [1], large electromechanical coupling coefficients [2], exhibit pyroelectric behavior and electroopic effects [3]. Potential applications [4] include optical shutters and modulators, transducers, displays, ferroelectric gate FET's, and many others. To date, most PZT thin films have been prepared by vacuum methods, including flash [5] and electron beam evaporation [6], rf diode [7] or magnetron [8] sputtering, and ion-beam deposition [9]. Common difficulties associated with these techniques include: lower resistivities, lack of compositional control, lower values of dielectric permittivity and spontaneous polarization when compared with bulk materials, and nonuniformity in thickness with cracking.

Manuscript received February 25, 1987; accepted March 9, 1987. This work supported by the US Department of Energy, Division of Materials Sciences, under contract DE-ACO2-76ER01198.

The authors are with the Department of Ceramic Engineering, University of Illinois, 105 S. Goodwin Ave., Urbana, IL 61801.

IEEE Log Number 8717135.

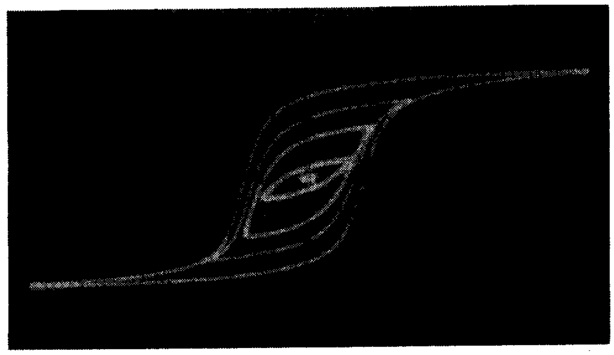

Fig. 1: Typical family of step-by-step P-E hysteresis loops obtained from 1-μm thin film of PZT on platinum. Scale per large division; x-axis: electric field (E) 5.10^6 V/m; y-axis: polarization (P) 0.33 C/m^2.

Recently, the fabrication of Pb-based perovskites, which include PZT and PLTZ thin-films, have been reported by sol-gel methods [10]. The technique has been refined to form films with dielectric strengths in excess of 100 V/μm, with compositionally adjustable relative permittivities of 1200 or greater. The dielectric properties of these thin-films are comparable with literature values reported for dense bulk materials [11], [12]. The present paper reports on recently measured ferroelectric hysteresis properties determined for sol-gel derived Pb $(Zr_{0.53}Ti_{0.47})O_3$ (PZT 53/47) thin films.

Materials and Methods

PZT solutions were prepared by reacting Pb acetate with Zr and Ti propoxides in methoxyethanol. Details of this procedure is given elsewhere [12]. Thin-films were spin cast from 0.5 molar solutions at 2000 r/min on platinum substrates using a photoresist spinner. The films were sintered in air for 10 min. at 650°C having a final fired thickness of 1 μm. Gold electrodes were patterned directly onto the films (0.175 mm square arrays) by sputtering for proper electrical contact. Ferroelectric measurements were made on a modified Sawyer–Tower bridge [13] having compensation capabilities.

Conclusion

Fig. 1 illustrates a typical family of polarization–field (P–E) loops generated at 50 Hz. from a 1-μm thin film of PZT on platinum. By exposing the camera film every time the applied field was increased, a step-by-step elongation of the hysteresis loop was obtained. These gel-derived thin-films did not break down during attempts to saturate the polarization, indicating suitability for devices based on ferroelectric switching. A remanent polarization (P_r) of 0.36 C/m^2, was measured, with a coercive field (E_c) of 4.10^6 V/m. The values are somewhat greater than data reported in the literature [6], [7], [9]. In particular, P_r for sol-gel derived PZT films was significantly greater than the highest value of P_r (0.31 C/m^2) reported to date [14] for a 2-μm organometallic-derived film, sintered at 700° C.

From a device point of view, the sol-gel processing route represents an alternative to thin film dielectric manufacture. Detailed studies on the switching and stability characteristics of these films are in progress and will be reported in due time.

0885-3010/88/0100-0080$01.00 © 1988 IEEE

References

[1] B. Jaffe, W. R. Cook, and H. Jaffe, *Piezoelectric Ceramics*. New York: Academic, pp. 135–183, 1970.

[2] K. Suzuki and M. Nishikawa, "Poling dependence of the surface-wave frequency-generation on PZT," *Jap. J. Appl. Phys.*, vol. 13, pp. 240–243, 1974.

[3] C. E. Land, P. D. Thatcher, and G. H. Haertling, "Electrooptic ceramics," in *Appl. Solid State Sci.*, vol. 4, R. Wolfe, Ed. New York: Academic, pp. 137–233, 1974.

[4] J. C. Burfoot and G. W. Taylor, *Polar Dielectrics and their applications*. Berkeley and Los Angeles: Univ. Calif., 1979.

[5] L. S. Phillips, "Ferroelectric films by flash evaporation of PZT," *Electron. Comp.*, vol. 12, pp. 523–526, 1971.

[6] M. Oikawa and K. Toda, "Preparation of $Pb(Zr, Ti)O_3$ thin films by an electron beam evaporation technique," *Appl. Phys. Letters*, vol. 29, pp. 491–492, 1976.

[7] A. Okada, "Electrical properties of lead zirconate-lead titanate thin films and their composition analysis by auger electron spectroscopy," *J. Appl. Phys.*, vol. 49, pp. 4494–4499, 1978.

[8] S. B. Krupanidhi, N. Maffei, M. Sayer, and K. El-Assal, "rf planar magnetron sputtering and characterization of ferroelectric $Pb(Zr, Ti)O_3$ films," *J. Appl. Phys.*, vol. 54, pp. 6601–6609, 1983.

[9] R. N. Castellano and L. G. Feinstein, "Ion-beam deposition of ferroelectric lead zirconate titanate (PZT)," *J. Appl. Phys.*, vol. 50, pp. 4406–4411, 1971.

[10] K. D. Budd, S. K. Dey, and D. A. Payne, "Sol-gel processing of $PbTiO_3$, $PbZrO_3$, PZT and PLZT thin films," in *Brit. Cer. Soc. Proc.*, vol. 36, 1985, pp. 107–121.

[11] S. K. Dey, K. D. Budd and D. A. Payne, "Characteristics of chemically-derived lead perovskite dielectric layers for high speed switching VLSI chips," in *Symp. Electronics Packaging and Materials Science, Mater. Res. Soc.* Palo Alto, CA, Apr. 1986.

[12] K. D. Budd, S. K. Dey and D. A. Payne, "The effect of hydrolysis conditions on the characteristics of $PbTiO_3$ gels and thin films," in *Better Ceramics Through Chemistry II*, vol. 73, Pittsburgh: Materials Research Society, pp. 711–716, 1986.

[13] B. A. Tuttle, "Polarization reversal and electrocaloric measurements for field-enforced transitions in the system lead zirconate-lead titanate-lead oxide: Tin oxide," Ph.D. Thesis, Univ. Ill. at Urbana-Champaign, pp. 85–87, 1981.

[14] J. Fukushima, K. Kodaira and T. Matsushita, "Preparation of ferroelectric PZT films by thermal decomposition of organometallic compounds," *J. Mater. Sci.*, vol. 19, pp. 595–598, 1984.